Formation of oxygen vacancies and charge carriers induced in the *n*-type interface of a $LaAlO_3$ overlayer on $SrTiO_3$(001)

Yun Li,[1] Sutassana Na Phattalung,[2] Sukit Limpijumnong,[2] Jiyeon Kim,[1] and Jaejun Yu[1,*]

[1]*Department of Physics and Astronomy, FPRD, Center for Strongly Correlated Materials Research, Seoul National University, Seoul 151-747, Korea*

[2]*School of Physics, Suranaree University of Technology, Synchrotron Light Research Institute, Nakhon Ratchasima 30000, Thailand*

(Received 5 August 2011; revised manuscript received 22 November 2011; published 12 December 2011)

We investigate the formation mechanism of oxygen vacancies and the properties of charge carriers induced in the *n*-type interface of a $LaAlO_3$ (LAO) overlayer on $SrTiO_3$(001) (STO) by carrying out density-functional-theory (DFT) calculations. We find that the formation of a low concentration of oxygen vacancies is dominated by the coupling between oxygen vacancies and the polar electric field in LAO. Oxygen vacancies on the LAO surface, which maximally reduce the electrostatic energy in LAO, are energetically the most stable, and most of the charge carriers induced by the surface vacancies are confined to the interface, forming a two-dimensional electron gas. We also verify that a high concentration of oxygen vacancies in the STO substrate could give rise to a three-dimensional electron gas. In addition, we demonstrate that the band profile at the interface is mainly determined by the concentration of the surface oxygen vacancies.

DOI: 10.1103/PhysRevB.84.245307 PACS number(s): 68.35.−p, 73.20.−r

I. INTRODUCTION

Since Ohtomo and Hwang reported the existence of a high-mobility electron gas at the *n*-type $(LaO)^+/(TiO_2)^0$ interface between two band insulators LAO and STO,[1] many properties associated with the electron gas at this interface, such as metal-insulator transition,[2–5] superconductivity,[6,7] and ferromagnetism,[8] have been observed. The origin of the electron gas at this interface and its potential device applications has attracted much interest. One formation mechanism of the electron gas which has been the most extensively studied is the so-called electronic reconstruction, in which a charge of 0.5 electrons per unit-cell area (e/A) transfers from LAO to STO to avoid the electrostatic potential divergence produced by the polar electric field in LAO.[1,9]

Two kinds of doping mechanisms, intrinsic and extrinsic doping, are involved with collaborating with the electronic reconstruction in the formation of the electron gas in the LAO/STO interface structure. In stoichiometric structures the charge carriers are generated by the intrinsic doping,[2,3] i.e., the electrons transfer from the LAO valence band to the STO conduction band. For instance, in the structure with an LAO overlay on STO(001) the electronic reconstruction results in a two-dimensional electron gas at the interface when the LAO thickness exceeds three unit-cell layers.[2,10,11] But, the density of this electron gas is far less than 0.5 e/A because ionic polarization partly screens the polar electric field in LAO.[2,8,10–13] In contrast, the extrinsic doping, in the form of oxygen vacancies, could generate the carriers with a density varying in a wide range, e.g., from 0.5 e/A to three orders of magnitude larger than this value.[1,8,14–17] It has been pointed out that in the LAO/STO superlattice the carriers of 0.5 e/A at the *n*-type interface can be generated by 0.25 oxygen vacancies per unit-cell area at the *p*-type interface.[9,14,19] While, the high carrier density, far beyond the value of 0.5 e/A predicted by the electronic reconstruction, was ascribed to a high concentration of oxygen vacancies in the STO substrate, and such carriers show a three-dimensional distribution and high mobility.[10,15,16] Remarkably, it was found in a recent experiment that in the same sample of LAO/STO interface the carriers generated by oxygen vacancies display diverse mobilities, in which the carriers in the bulk region of STO substrate have a higher mobility than those in the interface region.[18] This varying dimensionality and mobility of the charge carriers induced by oxygen vacancies in the LAO/STO interface structure has not been fully understood.

Up to now, most works about oxygen vacancies in the LAO/STO interface structure focused on the STO substrate. Whether oxygen vacancies exist in LAO is still unknown. In addition, the electronic properties of oxygen vacancies in LAO and the distribution character of the induced charge carriers needs more investigation. In this paper, we present a comprehensive study for the formation mechanism of oxygen vacancies and the properties of charge carriers induced in the *n*-type interface of an LAO overlayer on STO(001) by carrying out DFT calculations. First, we calculate the formation energies of various concentrations of oxygen vacancies and demonstrate how the polar electric field in LAO affects the formation of oxygen vacancies. Then, we explore the carrier properties, including polarity compensation, density and dimensionality. Finally, we discuss the conducting properties of the carriers and present the band profiles corresponding to various concentrations of oxygen vacancies.

II. COMPUTATIONAL METHOD

We carried out the DFT calculations within a generalized gradient approximation (GGA)[21] together with the projector augmented wave method[22,23] and a kinetic energy cutoff of 400 eV as implemented in the Vienna *ab initio* simulation package (VASP).[20] We modeled the *n*-type LAO/STO interface into a supercell consisting of a STO(001) substrate, an LAO overlayer on it and a vacuum region of about 14 Å. In all calculations for the formation energies of oxygen vacancies and the carrier densities, we used seven unit-cell layers of

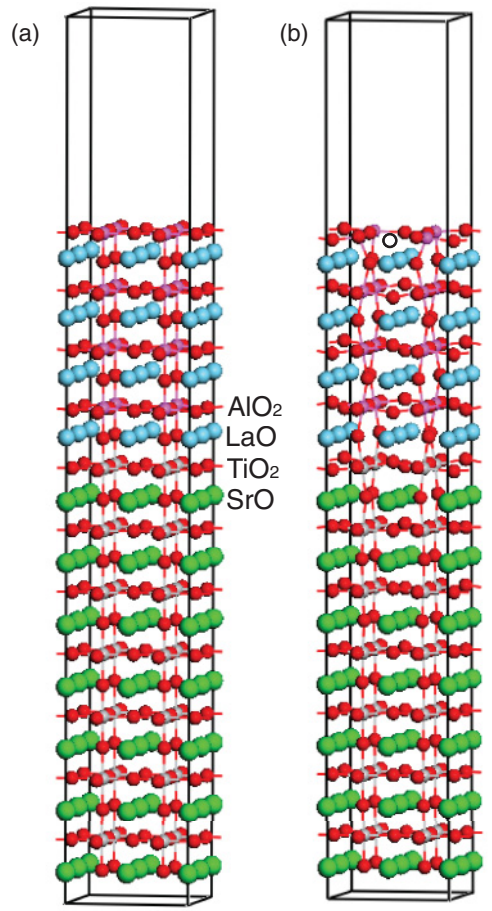

FIG. 1. (Color online) (2 × 2) supercells to model the n-type interface of an LAO overlayer on STO(001) (a) without oxygen vacancy and (b) with one oxygen vacancy (black circle) on the LAO surface.

STO substrate, with which the results are sufficiently accurate in comparison with a much thicker one. Dipole correction was employed to cancel the errors of electrostatic potential, atomic force and total energy, which are caused by periodic boundary condition.[24] To simulate various concentrations of oxygen vacancies, we used (2×2), (3×2), and (3×3) in-plane supercells, and sampled the Brillouin zone with Γ-centered (5×5), (3×5), and (3×3) **k**-point meshes, respectively. Figures 1(a) and 1(b) display a relaxed (2×2) supercell without oxygen vacancy and one with one oxygen vacancy on the LAO surface. The in-plane lattice constant of the slab was constrained at the calculated equilibrium value of STO bulk ($a = 3.942$ Å). All coordinates of atomic positions were fully relaxed until the atomic forces were less than 0.02 eV/Å except for the atoms in the bottom two layers of STO, which were fixed in their bulk positions.

III. ENERGETIC STABILITIES OF VARIOUS CONCENTRATIONS OF OXYGEN VACANCIES

For simplification, we denote the concentration of oxygen vacancies and the density of charge carriers as n_V and n_e in the unites of $1/A$ and e/A, respectively. It was pointed out that the charge of 0.5 e/A transferred from the LAO surface to STO can completely compensate the polar electric field in LAO.[9] For oxygen-vacancy doping, this charge density corresponds to 0.25 oxygen vacancies per unit-cell area, i.e., $n_V = 0.25$. To comprehensively understand the formation of oxygen vacancies and the properties of induced carriers, we studied three concentration regimes of oxygen vacancies, $n_V < 0.25$, $n_V = 0.25$, and $n_V > 0.25$, which were simulated by introducing one oxygen vacancy in (3×2) and (3×3) supercells, one in (2×2), and two in (2×2), respectively. To compare the stabilities of various oxygen-vacancy configurations, we used the following formula of formation energy of oxygen vacancies at the oxygen-rich limit:

$$E_f = E_V - (E_0 - n \cdot 0.5E_{O_2}),$$

where E_V, E_0 are the total energies of the interface structure with and without oxygen vacancies, $0.5E_{O_2}$ is the chemical potential of an oxygen atom at the oxygen-rich limit, and n is the number of oxygen vacancies.

Figure 2 displays the formation energies for various concentrations of oxygen vacancies. For $n_V < 0.25$ and $n_V = 0.25$, the formation energies exhibit clear dependence on the location of the oxygen vacancy: (I) Oxygen vacancy on the LAO surface layer always has the lowest formation energy;[25] (II) The formation energies of oxygen vacancies in the AlO_2 layers approximately decrease linearly from the interface to the surface; (III) The formation energies of oxygen vacancies in LAO are always lower than in STO. These behaviors are accounted for by the coupling between the polar electric field in LAO and the oxygen vacancies. Our electronic structure calculations (see the following section) show that a charge of no more than 0.5 e/A, doped by oxygen vacancies in LAO, transfers to STO because of the polar electric field in LAO. For an oxygen vacancy on the LAO surface, the charge transferring compensates the polar electric field in the entire LAO overlayer, maximally lowering the electrostatic energy in LAO. However, for an oxygen vacancy in the LAO layers below the surface, the charge transferring only compensates the polar electric field in the region from the oxygen-vacancy

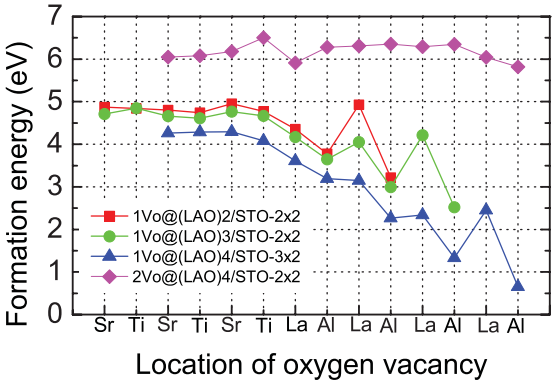

FIG. 2. (Color online) Formation energies of oxygen vacancies at different atomic layers in the LAO/STO interface structure. The legend of 1Vo@(LAO)2/STO-2×2 stands for one oxygen vacancy in a (2×2) supercell containing two LAO layers, others follow the same convention. For the (2×2) supercell containing two oxygen vacancies, one is fixed on the LAO surface and the other varies at different atomic layers. Atomic layers of SrO, TiO_2, LaO, and AlO_2 are denoted as Sr, Ti, La, and Al, respectively.

layer to the interface. On the contrary, the charge doped by an oxygen vacancy in STO has little effect on compensating the polar electric field because of no charge transferring from LAO to STO. The linearity of the formation energies of oxygen vacancies in the AlO_2 layers just reflects the approximate constant strength of the polar electric field. In addition, one might notice that the formation energies of oxygen vacancies in LaO layers are largely higher than in the AlO_2 layers. We found that this is due to the out-of-plane compressive distortion in LAO raised by the polar electric filed. With this distortion, two Al ions connected along the out-of-plane direction with the oxygen vacancy in the LaO layer have a shorter distance and therefore a larger Coulomb repulsive energy than those along the in-plane direction with the oxygen vacancy in the AlO_2 layer. Moreover, this kind of distortion and the resulting energy difference of the oxygen vacancy in the LaO and in the AlO_2 layer are stronger in the surface layer than in the interface layer.

For $n_V = 0.25$, the formation energy of the oxygen vacancy on the LAO surface is also dependent on the LAO thickness. As shown in Fig. 3, at a given value of the chemical potential of the oxygen atom, the formation energy decreases proportionally with the LAO thickness increasing from 2 to 4 unit-cell layers, and seems to be almost unchanged after four layers. This behavior reflects the variation of the difference between the electrostatic energy in the ideal LAO/STO structure and that in the oxygen-vacancy structure with increasing LAO thickness. In the ideal structure with less than four layers of LAO, no intrinsic doping occurs so that the electrostatic energy increases with increasing LAO thickness. In contrast, in the structure with surface oxygen vacancies the electrostatic energy completely vanishes. So the difference of electrostatic energies in these two structures increases with increasing LAO thickness. However, once the LAO thickness of the ideal structure exceeds four layers, the electronic reconstruction eliminates the increment of electrostatic energy induced by more LAO layers.[12,13,26] Thus, the difference of electrostatic energies does not increases, i.e., the formation energy of oxygen vacancy remains unchanged with increasing LAO thickness. Besides, at the oxygen-rich limit the ideal structure is always more stable than oxygen-vacancy structure, implying that even with a very thick LAO layer the vacancy-free

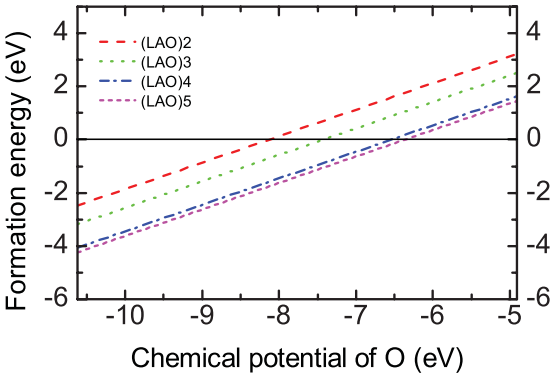

FIG. 3. (Color online) Formation energies of one oxygen vacancy on the LAO surface of (2×2) supercells as a function of the chemical potential of the oxygen atom. The LAO thicknesses vary from 2 to 5 unit-cell layers. The ideal structure is the reference.

interface structure still can be fabricated with high oxygen pressure; while with low oxygen pressure corresponding to the low chemical potential in Fig. 3, the oxygen-vacancy structure becomes more stable than the ideal one. This is consistent with the experimental results.[2,8,10,11]

For $n_V > 0.25$, we fixed one oxygen vacancy on the LAO surface and varied the other at different atomic layers. The formation energies are also presented in Fig. 2. In contrast to $n_V \leqslant 0.25$, for $n_V > 0.25$ the formation energy of the extra oxygen vacancy does not show apparent position preference because the polar electric field is completely compensated by the oxygen vacancy on the LAO surface. This implies that with low oxygen pressure, besides on LAO surface, oxygen vacancies can be formed in any atomic layer.

IV. ELECTRONIC STRUCTURES OF OXYGEN VACANCIES

First we focus on the electronic structure of oxygen vacancy of $n_V < 0.25$ on LAO surface. In the layer-projected density of states (LPDOS) shown in Fig. 4, an empty localized oxygen-vacancy state appears slightly below the conduction band minimum (CBM) of LAO surface layer. Since the energy level of this oxygen-vacancy state is higher than the STO CBM, both electrons in this state transfer to the conduction band of STO. As the density of the transferred charge is less than $0.5\ e/A$, the polar electric field in LAO is only partly compensated. The residual polar electric field leads to an upward band-shift from the interface to the LAO surface and ionic displacements in LAO, as shown in Figs. 4(a) and 4(c).

Moreover, for $n_V < 0.25$ the LAO thickness is another factor determining the carrier density at the interface. For a given concentration of oxygen vacancies, the valence band maximum (VBM) of the LAO surface layer shifts upward with the LAO thickness increasing until to a critical thickness

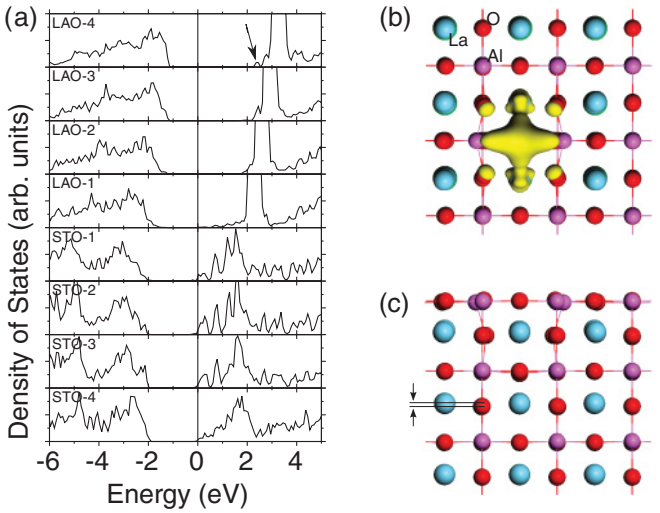

FIG. 4. (Color online) (a) Layer-projected density of states of (3×3) supercell with one oxygen vacancy on the LAO surface. The arrow points to the oxygen-vacancy state. (b) Top view of the spatial distribution of the oxygen-vacancy state at the surface. (c) Side view of the top three LAO layers. The arrows and horizontal lines denote the ionic displacement in LAO.

(t_c) of which the VBM of the LAO surface layer just exceeds the STO CBM. Once the LAO thickness exceeds the critical thickness, a charge in the valence band of the LAO surface layer will transfer to the conduction band of STO. This means that both extrinsic and intrinsic doping contribute to the carrier formation. Based on this electrostatics picture, we derived an expression for the carrier density n_c as the function of the concentration of oxygen vacancies n_V and LAO thickness t,

$$n_c = \begin{cases} 0.5 - \frac{A}{t - t_0} & t > t_c \\ 2n_V & t \leqslant t_c \end{cases}, \quad (1)$$

$$t_c = \frac{A}{0.5 - 2n_V} + t_0, \quad (2)$$

where $A = 1.97$ and $t_0 = 0.053$ are from our previous DFT study,[13] t and t_0 are in the unit of unit-cell layer. For a (3×3) supercell with one vacancy on the surface, the critical thickness is 7.1 unit-cell layers from above formula, which is in good agreement with our DFT-calculated value, seven unit-cell layers.

For $n_V = 0.25$, the configuration with one oxygen vacancy on the LAO surface has the lowest total energy, while that with one oxygen vacancy in STO has the highest total energy. Figure 5 displays the LPDOSs of these two configurations. In the former, where the calculated carrier density at the interface is 0.5 e/A, the polar electric field in LAO is completely compensated, resulting in a straight alignment of the VBMs of LAO layers. On the contrary, in the latter the upward band-shift in LAO still remains although the carrier density is also 0.5 e/A. This indicates that the carrier charge induced by oxygen vacancies in STO hardly compensates the polar electric field in the LAO overlayer.

For $n_V > 0.25$, the possible configuration is that one oxygen vacancy lies on the LAO surface and the other in any atomic layer. Figure 6 displays the LPDOSs of two configurations with both oxygen vacancies in LAO. Although the details of oxygen-vacancy states in these two configurations are different, the densities of the charge transferred from the oxygen-vacancy state to STO are both equal to 0.5 e/A. Moreover, other configurations with two oxygen vacancies in LAO also show the same carrier density in STO. These results indicate that oxygen vacancies in LAO can contribute at most 0.5 electron carriers per unit-cell area in STO. The reason is that the transferred charge of 0.5 e/A completely compensated the polar electric field in LAO, any additional charge transferring would set up an inverse electrostatic field in LAO, leading to a rising of electrostatic energy. For the configurations with one oxygen vacancy on the LAO surface and the other in STO, the oxygen vacancy in STO just increases the carrier density, but does not affect the band shape.

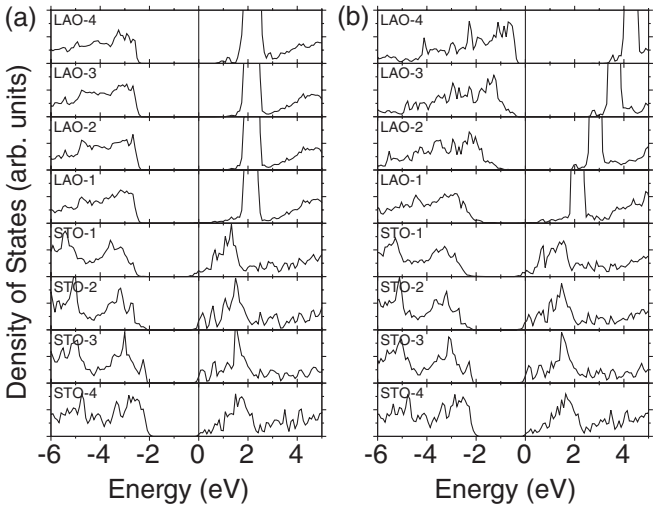

FIG. 5. Layer-projected DOSs for (2×2) supercells (a) with one oxygen vacancy on the LAO surface and (b) with one oxygen vacancy in STO-1 layer.

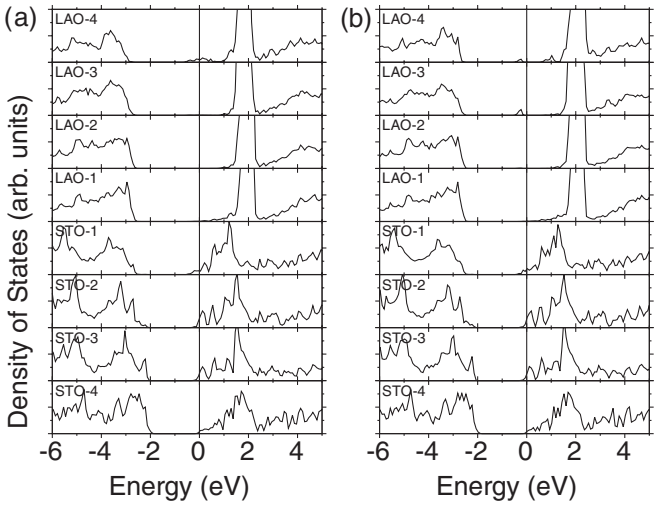

FIG. 6. Layer-projected DOSs for (2×2) supercells (a) with two oxygen vacancies on the LAO surface and (b) with one vacancy on the LAO surface and the other in the LAO-3 layer.

V. DISCUSSION

A. Dimensionality of carrier distribution

In order to explore the dimensionality of the carriers induced by oxygen vacancies, we performed DFT calculations by employing a (2 × 1) supercell containing a 17 unit-cell layers of STO. For $n_c < 0.5$, since the density and origin of the charge carriers is similar to the case of intrinsic doping in which a charge with the density of less than 0.5 e/A transfers from the LAO surface to STO and is confined within about three layers at the interface,[11,13] a similar potential profile and resulting carrier distribution at the interface as that of the case of intrinsic doping should also appear. Therefore, here we only focus on the cases of $n_c = 0.5$ and $n_c > 0.5$. The carrier densities of $n_c = 0.5$ and $n_c > 0.5$ were obtained by introducing one oxygen vacancy on the LAO surface and by two vacancies of which one is still on the LAO surface and the other is in the middle of the STO substrate. Figures 7(a) and 7(b) illustrate the distribution of the carriers of $n_c = 0.5$ in the STO substrate. Apparently, most carriers accumulate at the interface within three unit-cell layers and mainly occupy the Ti d_{xy} orbital, showing a two-dimensional distribution. The rest extend far from the interface and occupy all three t_{2g} orbitals. This orbital anisotropy at the LAO/STO interface has been demonstrated to be raised by the strong in-plane hybridization

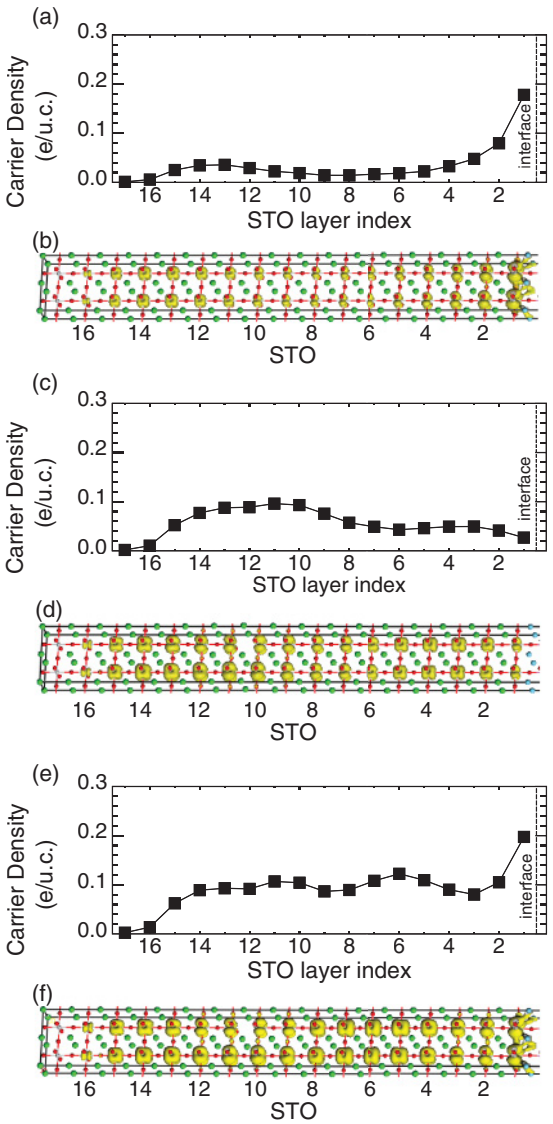

FIG. 7. (Color online) Layer-resolved density and spatial distribution of charge carriers in the $(LAO)_3/(STO)_{17}$-(2×1) supercell with oxygen vacancies. (a), (b) For one oxygen vacancy on the LAO surface; (c), (d) for one oxygen vacancy in the middle of STO; (e), (f) for one oxygen vacancy on the LAO surface and another in the middle of STO. LAO at right side of STO is omitted. The unit of carrier density is electron per unit cell.

among d_{xy} orbitals and the out-of-plane compressive distortion of TiO_6 octahedrons at the interface.[13,27,28] Furthermore, we also present the distribution of the carriers induced by one oxygen vacancy in the middle of the STO substrate in Figs. 7(e) and 7(f). The carrier confinement at the interface disappears, instead, the carriers almost evenly distribute in the whole STO substrate. This indicates that without the charge transferring from LAO to STO the two-dimensional carriers can not be formed.

Figures 7(c) and 7(d) illustrate the distribution of the carriers of $n_c > 0.5$. Clearly, the carriers consist of two parts: One is still confined to the interface within three unit-cell layers and mainly occupies the Ti d_{xy} orbital; The other extends in the whole STO substrate and occupies all three t_{2g} orbitals. Since the carriers confined to the interface vanish the polarity discontinuity, the distribution of the carriers induced by the oxygen vacancies in the STO substrate is similar to that in an individual STO bulk, where oxygen vacancies generally generate a well-extended electron gas.[29] This implies that a high concentration of oxygen vacancies in the LAO/STO interface structure will give rise to a three-dimensional electron gas in the STO substrate.

The above calculated carrier distributions agree well with the experimental results measured by using conducting atomic forcer microscopy, in which the carriers show a two-dimensional distribution in the sample grown at high oxygen pressure and a three-dimensional distribution in that at low oxygen pressure.[10] This varying dimensionality of carrier distribution provides us a way to explain the diversity of carrier mobility observed in the experiments. For the two-dimensional carriers, the mobility might be reduced by two factors: the dislocations, which has been observed at the LAO/STO interface and may strongly trap or scatter the carriers,[9,30] and the strong correlation effect of Ti d electrons at the interface layers, with which the carriers might be localized into a narrow Hubbard band and thus have a large effective mass.[31,32] However, the extended parts of the three-dimensional carriers are not affected by the above two factors, and thus have a higher mobility.

B. Band diagrams

Based on above calculated electronic structures, we plotted schematic band diagrams of the LAO/STO interface with various concentrations of oxygen vacancies, shown in Fig. 8. All configurations exhibit a strong band bending at the interface on the STO side because of charge transferring from the LAO surface to STO. On the LAO side the band shapes are dominated by the concentration of oxygen vacancies on the LAO surface. For $n_V < 0.25$ ($n_c < 0.5$), the polar electric field in LAO is partly compensated, the residual field results in a band sloping [Fig. 8(a)]. While for $n_V = 0.25$ ($n_c = 0.5$), the polar field is completely compensated, resulting in flat

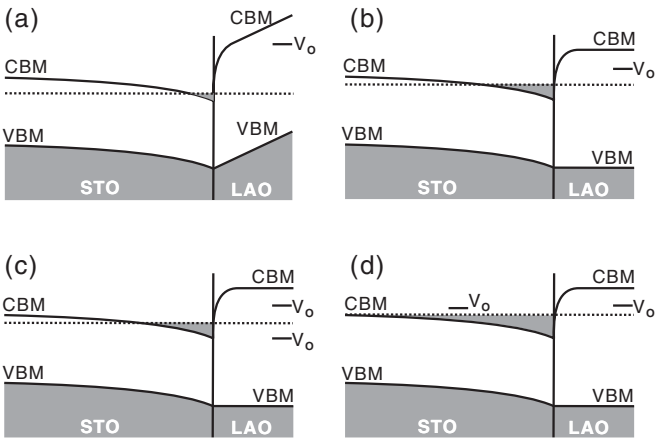

FIG. 8. Band diagrams of the LAO/STO interface with oxygen vacancies on the LAO surface for (a) $n_V < 0.25$, (b) $n_V = 0.25$, (c) $n_V > 0.25$, (d) $n_V > 0.25$ but oxygen vacancies in both the LAO surface layer and the STO substrate. Dashed line stands for Fermi level, and shade area for electron occupied states.

bands in LAO [Fig. 8(b)]. In the case of $n_V > 0.25$ [Fig. 8(c)] where all oxygen vacancies lie in LAO ($n_c = 0.5$), the band shape is the same as that of $n_V = 0.25$. In another case of $n_V > 0.25$ [Fig. 8(d)], the carrier density is larger than 0.5 e/A because of the oxygen vacancies in STO. Noticeably, all configurations of $n_V \geqslant 0.25$ show a flat VBM in LAO, which could be regarded as a marker of oxygen vacancies on the LAO surface. In addition, it should be noted that some localized states generated by oxygen-vacancy cluster or other vacancy cluster in STO[33,34] might appear in the band gap of the LAO/STO interface.

VI. SUMMARY

Using DFT calculations, we have studied the formation mechanism of different concentrations of oxygen vacancies and the properties of charge carriers induced in the LAO/STO interface. We show that a low concentration of oxygen vacancies are preferentially formed on the LAO surface, the electron gas induced by the surface oxygen vacancies exhibits a two-dimensional distribution at the interface and has a density upper limit, 0.5 electron per unit-cell area; while a high concentration of oxygen vacancies give rise to a three-dimensional electron gas in the STO substrate. Moreover, we also demonstrate that the band profile at the interface is mainly determined by the concentration of the surface oxygen vacancies.

ACKNOWLEDGMENTS

This work was supported by KOSEF through the ARP (R17-2008-033-01000-0) and by BK21. We acknowledge the support from KISTI under the Supercomputing Application Support Program. The authors thank Bo Xiong and Kelly Patton for carefully reviewing this manuscript.

*jyu@snu.ac.kr

[1] A. Ohtomo and H. Y. Hwang, Nature (London) **427**, 423 (2004).
[2] S. Thiel, G. Hammerl, A. Schmehl, C. W. Schneider, and J. Mannhart, Science **313**, 1942 (2006).
[3] M. Huijben, G. Rijnders, D. H. A. Blank, S. Bals, S. Van Aert, J. Verbeeck, G. Van Tendeloo, A. Brinkman, and H. Hilgenkamp, Nature Mater. **5**, 556 (2006).
[4] C. Cen, S. Thiel, G. Hammerl, C. W. Schneider, K. E. Andersen, C. S. Hellberg, J. Mannhart, and J. Levy, Nature Mater. **7**, 298 (2008).
[5] G. Rijnders and D. H. A. Blank, Nature Mater. **7**, 270 (2008).
[6] N. Reyren, S. Thiel, A. D. Caviglia, L. Fitting Kourkoutis, G. Hammerl, C. Richter, C. W. Schneider, T. Kopp, A.-S. Rüetschi, D. Jaccard, M. Gabay, D. A. Muller, J.-M. Triscone, and J. Mannhart, Science **317**, 1196 (2007).
[7] A. D. Caviglia, S. Gariglio, N. Reyren, D. Jaccard, T. Schneider, M. Gabay, S. Thiel, G. Hammerl, J. Mannhart, and J.-M. Triscone, Nature (London) **456**, 624 (2008).
[8] A. Brinkman, M. Huijben, M. Van Zalk, J. Huijben, U. Zeitler, J. C. Maan, W. G. Van der Wiel, G. Rijnders, D. H. A. Blank, and H. Hilgenkamp, Nature Mater. **6**, 493 (2007).
[9] N. Nakagawa, H. Y. Hwang, and D. A. Muller, Nature Mater. **5**, 204 (2006).
[10] M. Basletic, J.-L. Maurice, C. Carrétéro, G. Herranz, O. Copie, M. Bibes, É. Jacquet, K. Bouzehouane, S. Fusil, and A. Barthélémy, Nature Mater. **7**, 621 (2008).
[11] M. Sing, G. Berner, K. Goß, A. Müller, A. Ruff, A. Wetscherek, S. Thiel, J. Mannhart, S. A. Pauli, C. W. Schneider, P. R. Willmott, M. Gorgoi, F. Schäfers, and R. Claessen, Phys. Rev. Lett. **102**, 176805 (2009).
[12] R. Pentcheva and W. E. Pickett, Phys. Rev. Lett. **102**, 107602 (2009).
[13] Y. Li and J. Yu, J. Appl. Phys. **108**, 013701 (2010).
[14] J. N. Eckstein, Nature Mater. **6**, 473 (2007).
[15] G. Herranz, M. Basletić, M. Bibes, C. Carrétéro, E. Tafra, E. Jacquet, K. Bouzehouane, C. Deranlot, A. Hamzić, J.-M. Broto, A. Barthélémy, and A. Fert, Phys. Rev. Lett. **98**, 216803 (2007).
[16] A. Kalabukhov, R. Gunnarsson, J. Börjesson, E. Olsson, T. Claeson, and D. Winkler, Phys. Rev. B **75**, 121404 (2007).
[17] W. Siemons, G. Koster, H. Yamamoto, W. A. Harrison, G. Lucovsky, T. H. Geballe, D. H. A. Blank, and M. R. Beasley, Phys. Rev. Lett. **98**, 196802 (2007).
[18] S. S. A. Seo, Z. Marton, W. S. Choi, G. W. J. Hassink, D. H. A. Blank, H. Y. Hwang, T. W. Noh, T. Egami, and H. N. Lee, Appl. Phys. Lett. **95**, 082107 (2009).
[19] Z. Zhong, P. X. Xu, and P. J. Kelly, Phys. Rev. B **82**, 165127 (2010).
[20] G. Kresse and J. Furthmüller, Phys. Rev. B **54**, 11169 (1996).
[21] Y. Wang and J. P. Perdew, Phys. Rev. B **44**, 13298 (1991).
[22] P. E. Blöchl, Phys. Rev. B **50**, 17953 (1994).
[23] G. Kresse and D. Joubert, Phys. Rev. B **59**, 1758 (1999).
[24] G. Makov and M. C. Payne, Phys. Rev. B **51**, 4014 (1995).
[25] In most experiments, pulsed laser deposition or molecular beam epitaxy was used to grow the LAO/STO interface structure, an atomically flat LAO surface was formed.[8] Besides, to our knowledge, no evidence of the atomic reconstruction induced by oxygen vacancies on the LAO surface of the LAO/STO interface structure has been reported. So, the atomic reconstruction was not considered in our calculations.
[26] W. J. Son, E. Cho, B. Lee, J. Lee, and S. Han, Phys. Rev. B **79**, 245411 (2009).
[27] Z. S. Popović, S. Satpathy, and R. M. Martin, Phys. Rev. Lett. **101**, 256801 (2008).
[28] H. Chen, A. Kolpak, and S. Ismail-Beigi, Phys. Rev. B **82**, 085430 (2010).
[29] W. Luo, W. Duan, S. G. Louie, and M. L. Cohen, Phys. Rev. B **70**, 214109 (2004).
[30] A. S. Kalabukhov, Y. A. Boikov, I. T. Serenkov, V. I. Sakharov, V. N. Popok, R. Gunnarsson, J. Börjesson, N. Ljustina, E. Olsson, D. Winkler, and T. Claeson, Phys. Rev. Lett. **103**, 146101 (2009).
[31] R. Pentcheva and W. E. Pickett, Phys. Rev. Lett. **99**, 016802 (2007).
[32] J. S. Kim, S. S. A. Seo, M. F. Chisholm, R. K. Kremer, H.-U. Habermeier, B. Keimer, and H. N. Lee, Phys. Rev. B **82**, 201407 (2010).
[33] D. D. Cuong, B. Lee, K. M. Choi, H.-S. Ahn, S. Han, and J. Lee, Phys. Rev. Lett. **98**, 115503 (2007).
[34] Y. S. Kim, J. Kim, S. J. Moon, W. S. Choi, Y. J. Chang, J.-G. Yoon, J. Yu, J.-S. Chung, and T. W. Noh, Appl. Phys. Lett. **94**, 202906 (2009).